Inhalation Toxicology, 2011; 23(8): 468–475

ISSN 0895-8378 print/ISSN 1091-7691 online
DOI: 10.3109/08958378.2011.583944

informa
healthcare

RESEARCH ARTICLE

Binding of polystyrene and carbon black nanoparticles to blood serum proteins

Stefanie Fertsch-Gapp, Manuela Semmler-Behnke, Alexander Wenk, and Wolfgang G. Kreyling

Comprehensive Pneumology Center, Institute of Lung Biology and Disease and Focus Network Nanoparticles and Health, Helmholtz Zentrum München– Research Center for Environmental Health, Neuherberg/Munich, Germany

Abstract

Context: Once inhaled, nanoparticles (NP) deposit on the lung surface and have first contact with the epithelial lung lining fluid (ELF) rich in proteins, which may bind to NP.

Objective: In this study, we investigate the parameters that influence the binding between NP and proteins.

Materials and methods: We used the proteins albumin, transferrin (TF), and apolipoprotein A-1 (all known as proteins from ELF) and different NP (polystyrene NP with negative, positive, and neutral surface coatings, Printex G and Printex 90) as models.

Results: In all cases, a linear correlation of the added NP amount and the amount of bound proteins was found and was described quantitatively by binding indices. Bovine serum albumin (BSA), TF, and apo A-1 were bound to the largest extent to hydrophobic NP, which shows the extraordinary importance of the NP's surface properties.

Discussion: The binding index indicates the relevance of primary particle size and surface properties, including hydrophobicity.

Conclusion: Size and surface modifications of NP determine their protein binding. Our results suggest that the formation of conjugates of BSA, TF, and Apo A-1 with NP may play an important role in their translocation across the air–blood–barrier and subsequent biokinetics.

Keywords: Nanoparticles, Polystyrene, Elemental carbon Printex, Protein binding, Bovine serum albumin, Transferrin, Apolipoprotein A1, Binding index

Introduction

Inhaled nanoparticles (NP) are able to deposit in alveoli (Kreyling et al., 2006) of the human lung and the rat lung. It is known that they can penetrate the lung–blood barrier and accumulate in secondary target organs (Oberdörster et al., 2002; Kreyling et al., 2002; Oberdörster et al., 2005).

Because inhaled NP get in contact with the proteins of lung surfactant and the epithelial lung lining fluid (ELF) (Peters et al., 2006), it is possible that NP form complexes with these proteins (Geiser et al., 2005; Borm et al., 2006). In contrast to micrometer-sized particles, NP are similar in size to proteins or not much larger. These NP–protein complexes may play a crucial role in the penetration of the air–blood barrier into the circulation and the accumulation in other organs, when those proteins serve as ferry-boats carrying the NP across body membranes either transcellular and/or paracellular and within body fluids (Donaldson et al., 2004; Yang et al., 2005; Kreyling et al., 2007). Some serum proteins bind to many NP and others only to a few selected ones. Here, it would seem that not only the NP surface but also other NP properties such as hydrophobicity play an important role (Barrett et al., 1999). Furthermore, NP–protein conjugates may change when at low affinity, but highly abundant proteins are exchanged by less abundant but higher affinity proteins in the various body fluids and in intracellular fluids.

Address for Correspondence: Wolfgang G. Kreyling, Comprehensive Pneumology Center– Institute of Lung Biology + Disease, *Focus Network Nanoparticles and Health,* Helmholtz Zentrum München– Research Center for Environmental Health, Ingolstaedter Landstr. 1, 85764 Neuherberg/Munich, Germany. Tel: +49–89-3187-2309, Fax: +49–89-3187–3397. E-mail: kreyling@helmholtz-muenchen.de

(Received 18 February 2011; revised 08 April 2011; accepted 21 April 2011)

In experimental assays, conjugates of NP and proteins can be separated by centrifugation from free proteins in the solution (Kondo et al., 1991; Olivier et al., 1995; Barrett et al., 1999; Oliva et al., 2003; Rezwan et al., 2004; Semmler et al., 2004). The NP-bound proteins can be traced by separating and staining them on sodium dodecyl sulfate-polyacrylamide gel electrophoresis (SDS-PAGE) assays. Other authors describe an indirect differential quantification of NP–protein conjugates measuring the original protein concentrations versus the remaining free protein concentrations in the supernatant after removal of the NP–protein complexes (Kondo et al., 1991; Brown et al., 2000; Oliva et al., 2003). By using these methods, the purpose of this study was to characterize the binding of selected NP and proteins and to determine binding activities *in vitro*.

Materials and methods

We selected proteins that are not only essential in the epithelial lining fluid (ELF) but also in blood serum bovine serum albumin (BSA), transferrin (TF), and apolipoprotein A-1 (ApoA1) (Noël-Georis et al., 2002; Pieper et al., 2003). All proteins were purchased from Sigma-Aldrich, Munich, Germany. Albumin has a size of 66 kDa and the isoelectric point (IEP) is at pH 4.7 (Peters, 1996). In suspensions of neutral pH value, albumin is strongly negatively charged, but there are regions with neutral amino acids (Carter and Ho, 1994). TF has a size of about 80 kDa and an IEP at pH 5.6. It has a hydrophobic region in helix 5 (Sun et al., 1999). Apolipoprotein A-1 (apo A-1) has a size of 28 kDa (Cornelius et al., 2002), and its IEP is at pH 4.9–5.2 (Noël-Georis et al., 2002).

Polystyrene NP with neutral surface charge (PS–Plain–NP), polystyrene NP with carboxyl surface modification (PS–COOH–NP), and polystyrene NP with amino surface modification (PS–NH_2–NP) are monodisperse and have a mean diameter of 50 nm and a density of 1.03 g/cm^3. The surface concentrations of the carboxylated or aminated functional groups on PS–NP are 120 mmol/g NP. They were purchased from Postnova Analytics GmbH, Landsberg/Lech, Germany.

Printex 90 (primary particle diameter of 14 nm) and Printex G (primary particle diameter of 50 nm) have a bulk density of 1.8–1.9 g/cm^3. Their specific surface area is 300 and 30 m^2/g, respectively, according to the manufacturer. These carbon black NP, kindly provided by Evonik AG (formerly Degussa AG), Essen, were included in our study as polydisperse industrial NP of different sizes of the primary particles of these aggregates/agglomerates.

To detect the NP-bound proteins, we designed experiments in which we incubated NP and proteins, separated the bound proteins from the free proteins, and quantified them either by spectroscopy or by detecting them on SDS-PAGE gels.

Protein solutions (0.4 mg/ml) in phosphate-buffered saline (PBS) and NP at different concentrations were incubated 9:1 (v/v) at 37°C for 1 h under slow rotation (36 rotations per minute) on a roller ("RM 5", CAT M. Zipperer GmbH, Staufen, Germany). Incubation volumes of albumin and TF were 1 and 0.1 ml for Apo A-1. For each type of NP, we calculated the time necessary to let a single NP settle from the top of the fluid to the bottom. The following equations (Lottspeich et al., 1998) were used to:

$$\mathrm{sc} = \frac{d^2 \times (1-\varphi)(\rho_{NP} - \rho_{LM})}{18 \times \eta} \quad (1)$$

with: sc, sedimentation constant [S]; d, NP diameter [nm]; φ, bulking (can be assumed to be 0 in compact particles); ρ_{NP}, NP density [g/cm^3]; ρ_{LM}, solvent density [g/cm^3]; η, solvent viscosity [Pa·s]

and

$$t = \frac{\ln\left(\frac{r_{max}}{r_{min}}\right)}{\left(\omega^2 \times \mathrm{sc}\right)/10^{13}} \quad (2)$$

with:

t, centrifugation time [s]; r_{max}, maximal radius: distance from the bottom of the vial to the axis of rotation (according to manufacturer: 55 mm); r_{min}, minimal radius: distance from the meniscus of the fluid to the axis of rotation (calculated on the basis of a model); ω, angular speed $\omega = 2\pi u$; u, revolutions per second.

For solvent density and viscosity, the values of water at 23°C were used.

$\rho_{water,\ 23°C} = 0.998$ [g/ml]

$\eta_{water,\ 23°C} = 0.933$ [mPa·s]

The suspensions were centrifuged to separate the NP–protein–conjugates from the supernatant in the pellet (PS–NP: 85 min for a volume of 1 ml and 30 min for 100 µl suspensions; centrifugal force at the upper meniscus 8.1×10^4 and 12.3×10^4 g, respectively; Printex G: 30 min for a volume of 1 ml and 10 min for 100 µl suspensions; centrifugal force at the upper meniscus 1.18×10^4 and 1.42×10^4 g, respectively; Printex 90: 360 min for a volume of 1 ml and 25 min for 100 µl suspensions; centrifugal force at the upper meniscus 1.18×10^4 and 12.3×10^4 g, respectively). The supernatant contained the free proteins. The supernatant was decanted and kept for further analysis (see below). The pellet was washed three times using 1.5 ml respectively 100 µl PBS (Apo A-1). In each case, the washing fluid was decanted after centrifugation (81,000*g*, 20 min). Then, the pellet was resuspended in about 20 µl and transferred to a new cup. The samples were mixed with an SDS containing sample buffer (relation 1:2) and incubated for 5 min at 95°C. Then, an aliquot (3 µl) was put onto a 10% NuPAGE® Bis-Tris-Mini-Gel (Invitrogen™, Karlsruhe, Germany). Usually, the electrophoresis was run at a voltage of 200 V for 50 min. The SDS-PAGE was silver stained. The

electropherograms were analyzed with the "ImageJ" Software by densitometry (National Institute of Health; http://rsb.info.nih.gov/ij/) (Abramhoff et al., 2004)

Determination of NP diameter: dynamic light scattering

For determination of the PS–NP size distribution with or without bound proteins, the Malvern Particle Sizer (HPSS, Malvern Instruments, Herrenberg) was used. Therefore, the suspensions were resuspended briefly (3 min) in an ultrasonic bath and transferred (1 ml) in a transparent cuvette for measuring in the Particle Sizer.

Quantification of bound protein (depletion method)

The original protein suspension and the centrifuged supernatant were analyzed after incubation (before pellet washing) for protein concentration: the difference in protein content is due to the mass of protein bound to NP. For quantification of protein concentration, the Bio-Rad® protein assay was performed according to Brown et al. (2000). In a microwell plate, 5 µl protein solution and 200 µl of the 1:5 diluted and filtered Bio-Rad® dye solution were mixed. Each sample was analyzed in triplicate. After 15 min of incubation at room temperature, the optical density of the solution was determined with a microwell plate photometer (Labsystems iEMS Reader MF V2.2-0, Labsystems, Quickborn, Germany).

In case of the PS–NH_2–NP, we found that these NP could not be spun down completely and that obviously the few remaining NP (below 20 %) provided a photometric signal in the protein assay. This was proven in an assay with NP but without any protein, requiring a correction value to be subtracted from the photometric data. Centrifuging a PS–NH_2–NP suspension of 2 mg/ml concentration, the photometer signal corresponded to a protein concentration of 53 µg/ml, which is the correction value C_{corr}. In the case of lower original PS–NH_2–NP concentration, we reduced the correction value proportionally.

The percentage of protein bound to NP (BB) was determined by subtracting the depleted protein concentration (C_{dep}) in the supernatant from the original protein concentration C_{orig} without NP; in addition, the correction value (C_{corr}) was also subtracted, and this value was normalized to the original protein concentration C_{orig} without NP, see eq. (3):

$$BB = [C_{orig} - (C_{dep} - C_{corr})]/C_{orig} \times 100 \quad (3)$$

Influence of the pH value on the NP protein binding

In the pH range from 4.4 to 5.9, we used a citrate phosphate buffer system, and in the pH range from 6.9 to 8.4, a barbiturate buffer system, both with 0.8% NaCl according to Dulbecco's PBS. Data were obtained as described in the depletion method above.

Binding index

Protein (BSA, TF) solutions were incubated at different concentrations of NP ranging from 0.25 to 2 mg/ml. The NP concentrations were plotted against the percentage of the bound protein. The slope of a fitted trend line (forced through the origin of the coordinates) was defined to be the binding index (BI) and refers to the binding at pH 7.4 if not noted otherwise.

For comparison of NP with similar chemical characteristics but different primary particle size, we estimated the total surface area of the added NP and plotted this as the x-axis. From the fitted trend line over the NP surface area, the binding index $BI_{Surface}$ is relative to the NP surface area.

Estimate of the NP's surface coverage with proteins

We used the manufacturer's data referring to NP concentrations in the purchased dispersions. For BSA, we used the data given in the literature; in the case of TF and apolipoprotein A-1, we calculated the size using the Deep View/Swiss-PdbViewer 3.7 computer software (GlaxoSmithKline; http://www.expasy.org/spdbv/) (Guex and Peitsch, 1997):

Geometric dimensions

BSA: $(5.5 \times 5.5 \times 9)$ nm^3 (Rezwan et al., 2004)

Rezwan et al. used a heart-shaped model of BSA with regard to its domains with different net charge. The equilateral triangle model of BSA with triangular sides of 80 Å and a depth of 30 Å or 8.4 and 3.15 nm (Carter and Ho, 1994; Röcker et al., 2009) is only valid in x-ray crystallography and not in a solution according to Quinlan et al. (2005). Furthermore, one has to consider that the area which interacts finally with NP may be different again because of the extreme conformational flexibility of albumin (Carter and Ho, 1994). For our considerations, we chose the data by Rezwan et al. as a first approach, although there is a certain conflict with a study cited by Röcker et al., which confirmed the x-ray–based structure analysis of BSA also in solution (Ferrer et al., 2001).

TF: $(16.1 \times 8.0 \times 6.2)$ nm^3

Apolipoprotein A-1: $(10.8 \times 8.8 \times 2.5)$ nm^3

With known NP diameter D_p, density ρ_p and NP concentration C_p the particle number N_p can be calculated in the suspension:

$N_p = C_p/m_p$,

with $m_p = \rho_p \times \pi/6 \times D_p^3$

with m_p = mass per NP

From the known protein molecular weight MW_{prot} and protein number ($N_{Prot\,0.36}$) of the 0.36 mg/ml concentration, we can calculate the number of bound proteins ($N_{Prot/NP}$) per NP:

$$N_{Prot/NP} = N_{Prot\,bd}/N_p \quad (4)$$

With the number of bound protein molecules $N_{Prot\,bd}$ in the 0.36 mg/ml solution:

$N_{Prot\,bd} = BB/100 \times N_{Prot\,0.36}$

and the number of protein molecules $N_{Prot\ 0.36}$ in 0.36 mg/ml solution:

$N_{\text{Prot 0.36}} = m_{\text{prot}}/(\text{MW}_{\text{prot}} \times Z_{\text{avog}})$ $Z_{\text{avog}} = 6.022 \times 10^{23}$ (Avogadro number)

m_{prot} is the mass of incubated proteins.

With known lateral protein surface areas $SA_{\text{prot,I}}$ of the lateral side *i*, we also estimated the percentage F_{prot} of the total NP surface area (SA_{NP}) covered by the proteins, depending on the lateral side i of the protein adhering to the NP.

$$F_{\text{prot}} = (SA_{\text{prot,i}} \times N_{\text{Prot/NP}}/SA_{\text{NP}}) \times 100 \quad (5)$$

i = different lateral protein sides (e.g., $5.5 \times 5.5\,\text{nm}^2$ or $5.5 \times 9.5\,\text{nm}^2$ for albumin)

Results

Dynamic light scattering: influence of protein

The three monodisperse PS–NP with a nominal diameter of 50 nm were measured in PBS, and after incubation in BSA and TF solution, using dynamic light scattering in a Malvern Particle Sizer (Table 1; Figure 1). In addition, the hydrodynamic diameters of Printex 90 and Printex G with primary particle sizes of 14 and 50 nm, respectively, are shown in Table 1.

Influence of the NP's surface modification on protein binding

Densitometric analysis of the SDS-PAGE gels showed that the binding of BSA to different PS–NP (PS–Plain–NP, PS–COOH–NP, and PS–NH_2–NP) depends on the NP surface modification. The PS–Plain–NP bind a large amount of the BSA in the solution (Figure 2, lane 6) so that after centrifugation no more BSA was found in the supernatant (Figure 2, lane 2). It also shows that the PS–COOH and PS–NH_2 NP bind about 90% less BSA on their surface (Figure 2, lanes 7 and 8) and that the depletion of the protein solution compared with the control (Figure 2, lane 1) is much less in these NP (Figure 2, lanes 2 and 3).

Influence of the pH value

The PS–NPs' BSA binding capacity depending on the pH value is shown in Figure 3. The PS–COOH NP bound significantly more BSA at a pH value below 5.4 than above ($P < 0.05$) (Figure 3), whereas there is no difference for PS–Plain NP. Data for PS–NH_2–NP are not shown; binding was below 20% in all cases.

Influence of the NP concentration on the NP's binding capacity: BI

With the protein depletion method, linear dependencies of NP concentration and bound amounts of BSA and TF are shown in Figures 4 and 5, respectively, for all three PS–NP, with PS–Plain–NP showing a strong correlation. At a concentration of 2 mg/ml, the PS–Plain NP bind nearly all BSA, whereas both other PS–NP bind little BSA. The mass-dependent BI (BI_{Mass}, in units % (0.36 mg BSA)/mg NP) for the PS–Plain NP is almost 25 times and five times higher than for PS–COOH–NP and PS–NH2–NP, respectively (Table 2), indicating that hydrophobic NP bind better than hydrophilic NP. The BI_{Mass} of Printex 90 NP is highest for BSA and six-fold higher than that of Printex G NP with a 10-fold smaller surface area (Table 2). Comparing the BI_{Mass} of hydrophobic NP, they rank: Printex-90 NP > PS–Plain–NP > Printex-G NP. This corresponds at least qualitatively to their respective specific surface areas (Table 2).

BI_{Mass} for TF and Apo A-1 are generally similar to the BI_{Mass} of BSA showing highest BI_{Mass} for both hydrophobic NP: PS–Plain–NP and Printex-90 NP with large specific surface areas, whereas Printex-G NP shows consistently lower BI_{Mass}. Both charged hydrophilic PS–NP show low BI_{Mass}, and Apo A-1 does not bind to PS–NH_2–NP at all (Figure 6 and Table 2).

To analyze the role of the NP surface area, we introduced a BI_{Surface}. Table 2 shows the highest values of the PS–Plain–NP for all three proteins even though the specific surface area of Printex-90 NP is much larger. BI_{Surface} of both Printex NP do not differ as much as the BI_{Mass} for all three proteins. Now the values for Printex-G NP are consistently higher than those for Printex-90 NP, which may indicate some chemical differences on the surface of both NP.

Estimated NP surface coverage

Based on eq. (4), the number of BSA molecules bound per NP was calculated (Table 2). Supposing an unspecific binding, we assume that the proteins bind with their largest lateral side (see Methods section), which agrees with the data of Röcker et al. (2009). Eq. (5) was used to estimate the protein covered percentage of the surface area of a single NP: now Apo A-1 with the lowest molecular weight of the proteins covers the highest fraction of the NP surface area compared with the other NP (with the exemption of PS–NH2–NP, which did not

Table 1. Hydrodynamic diameters of PS–NP in PBS and BSA or transferrin solution (0.36 mg/ml), mean values of size distribution 10-fold measurements.

	Diameter in Distilled Water (nm)	Diameter in PBS (nm)	Diameter in BSA Solution (nm)	Diameter in Transferrin Solution (nm)
PS–Plain	70	50	1190	930
PS–COOH	110	110	110	110
PS–NH_2	170	110	90	90
Printex 90	50	>1000	n.d.	n.d.
Printex G	260	>1000	n.d.	n.d.

n.d., not determined.

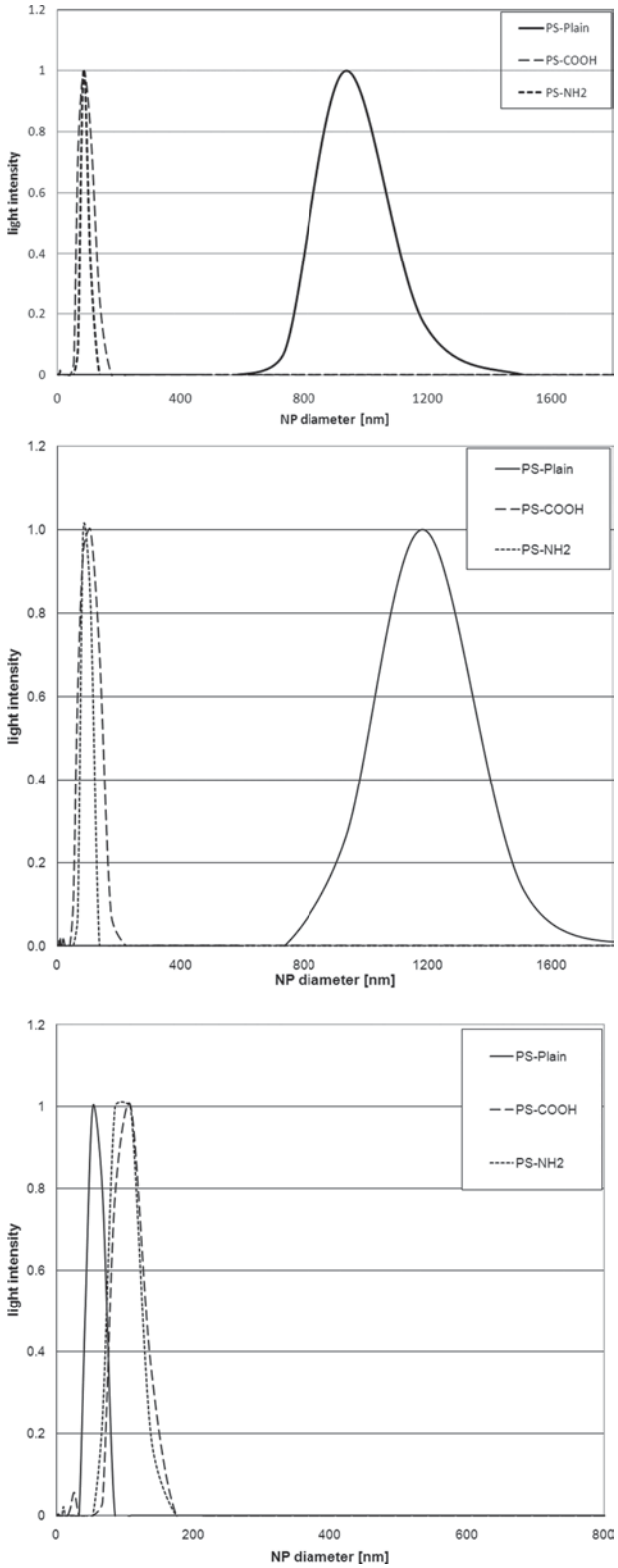

Figure 1. Size distribution measured by dynamic light scattering of all three polystyrene NP (2 mg/ml) suspended in PBS solution (top) and after incubation in BSA solution (middle) and transferrin solution (bottom). Average of 10 runs performed by the Malvern Particle Sizer HPSS. Note the abscissa in the top panel extends only half of the lower panels to allow visualization of the large size shift of the PS–Plain.

bind at all). In case of PS–Plain–NP, binding with the largest lateral side coverage is greater than 100% such that it is likely that one of the other lateral sides binds as well, unless double layers are formed. Here, we provide the covered percentage corresponding to the (8.8 × 2.5 nm) lateral side. Again, the hydrophobic NP

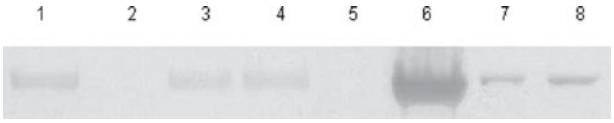

Figure 2. BSA amount in the supernatant and in the pellet after use of different PS–NP (0.2 mg/ml in 0.36 mg/ml BSA) and in the control (BSA solution with distilled water instead of dispersed NP): the supernatants contain free, not bound protein, and the pellets the bound proteins. Supernatants in lanes 1–4: lane 1, BSA and distilled water (control); lane 2, BSA and PS–Plain–NP; lane 3, BSA und PS–COOH–NP; lane 4, BSA und PS–NH_2–NP. Pellets in lanes 5–8: lane 5, BSA and distilled water (control); lane 6, BSA and PS–Plain–NP; lane 7, BSA and PS–COOH–NP; lane 8, BSA and PS–NH_2–NP.

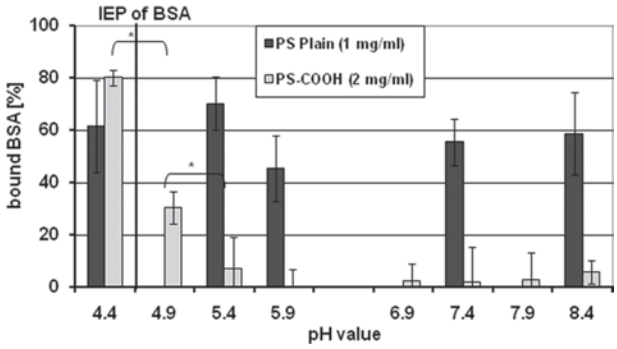

Figure 3. Binding of BSA (0.36 mg/ml) to PS–NP (PS–Plain–NP: 1 mg/ml, PS–COOH–NP and PS–NH_2–NP: 2 mg/ml) depending on the pH value ($n = 3$ for PS–Plain–NP and PS–COOH–NP, data for PS–NH_2–NP not shown, binding was below 20% in all cases, * with $P < 0.05$). IEP, isoelectric point.

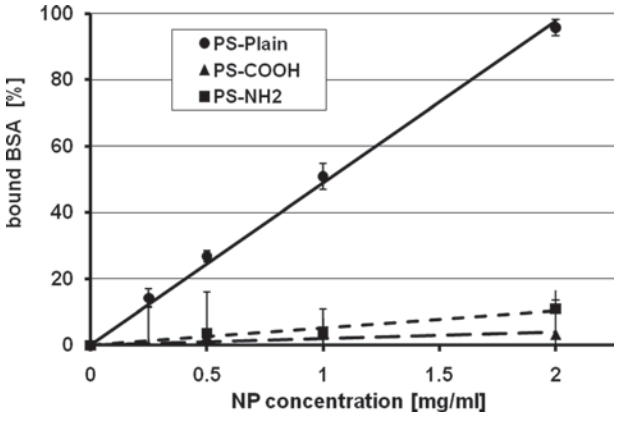

Figure 4. BSA depletion of the supernatant after separation of the NP protein complexes depending on the NP dose (0.25, 0.5, 1.0, and 2.0 mg/ml) ($n = 3$, the error bars show the standard deviation). Each line represents the linear regression, which was forced through the coordinate origin.

(PS–Plain–NP and both Printex NP) show highest coverages, and the differences between the two Printex NP are rather low. Surface coverage of the hydrophilic NP with BSA and TF are is rather low.

Discussion

At a pH value of 7.4, a linear correlation between NP amount and bound protein amount was found. The BI immediately describes the binding capacity of NP depending on their mass or surface area. Regarding the three different proteins the NP have specific binding patterns, which are in good agreement with the work of Lundqvist et al. (2008).

Further measurements showed that the extent of the agglomeration of PS–NP in the protein solution was influenced by their functional surface groups, and these data were related to the binding indices. Although the PS–Plain–NP formed a rather monodisperse solution (50 nm) in PBS, in the BSA solution, we found large agglomerates of up to 1200 nm hydrodynamic diameter, which indicates considerable BSA binding and subsequent agglomeration of NP and NP protein complexes. This agglomeration may be enhanced by the ability of BSA to form dimers (Rezwan et al., 2004). The hydrodynamic diameters of PS–COOH NP and PS–NH_2 NP were found to be larger than specified by the manufacturer, indicating that there was already agglomeration in PBS (see also Lundquist et al., 2008). The binding of BSA or TF did not change the size at all, which is in agreement with the low protein-binding capacities of those NP. Obviously, the proteins even inhibited agglomeration in these cases. Dimer formation of BSA is less probable because the PS–NH_2–NP bind only few proteins.

The extraordinary binding capacity of PS–Plain–NP could be also confirmed for Apo A-1 in our further experiments (Figure 6). Apo A-1 binds to all PS–NP in a rather similar pattern as BSA. TF binds highest to PS–Plain–NP and shows declining binding to the carboxylated and aminated NP, respectively.

Binding of all three proteins to the two hydrophobic carbon black NP demonstrates the importance of their primary particle size and hence their specific surface area. However, the strong surface curvature of small NP partially inhibits dense packaging of bound proteins (Cedervall et al., 2007), which is likely to explain the slightly lower $BI_{Surface}$ of Printex 90 of all three proteins compared with those of Printex G.

The high BSA-binding capacity of PS–NP was rather independent of the pH value, which indicates that the binding is driven by hydrophobic interactions. This is confirmed by other studies that already demonstrated the importance of hydrophobic interactions (Deng et al., 2009). The pH value of the solution also has no clear effect on the low binding capacity of the PS–NH_2–NP because it

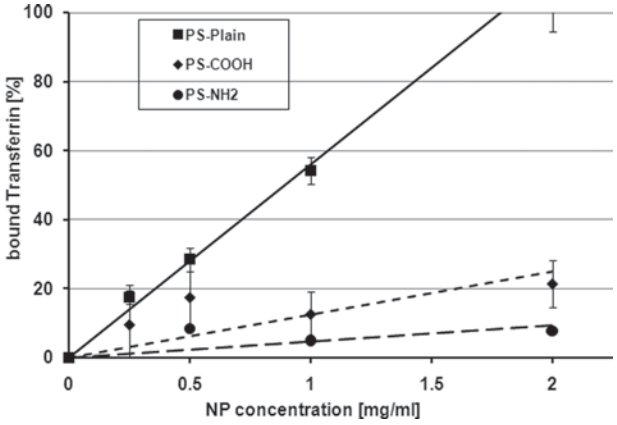

Figure 5. Transferrin depletion of the supernatant after separation of the NP protein complexes depending of the NP dose (0.25, 0.5, 1.0, and 2.0 mg/ml) ($n=3$, the error bars show the standard deviation). Each line represents the linear regression, which was forced through the coordinate origin.

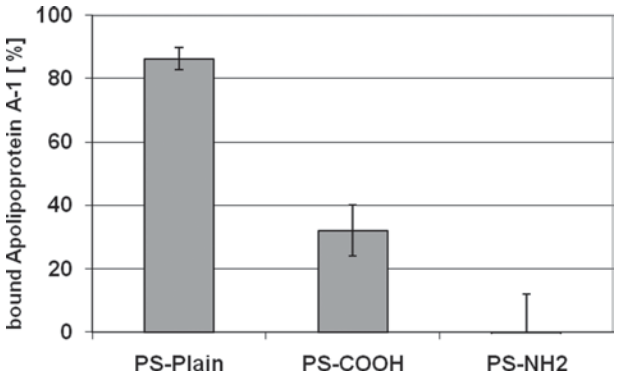

Figure 6. Binding of Apo A-1 (0.36 mg/ml) to different PS–NP at a concentration of 2 mg/ml depending on the surface modification of the NP; $n=3$; the error bars represent the standard deviation.

Table 2. Mass and surface area related to binding indices of the NP to different proteins.

	Diameter (nm)	Specific Surface Area (m^2/g)	BI_{Mass} (% protein/mg NP)			$BI_{Surface}$ (% protein/m^2 NP)			Surface Coverage (%)		
			BSA	Transferrin	Apo A-1	BSA	Transferrin	Apo A-1	BSA	Transferrin	Apo A-1
PS–Plain	50	120	49	56	43	407	466	359	66	~100	269/76
PS–COOH	50	120	2	13	13	17	104	116	<1	4	81/23
PS–NH_2	50	120	5	5	<0	44	39	< 0	<1	12	0
Printex G	50	30	9	12	11	313	398	360	~27	~62	~100%
Printex 90	14	300	62	57	42	205	269	139	~8	~71	~100%

Percentage relates to 0.36 mg BSA in the original solution. For Printex NP, the estimated surface coverage can only be a rough estimate because of the complex polydispersity of the primary NP and their agglomerates. For Apo A-1, the number before the slash shows the result when the protein adheres with its area of $10.8 \times 8.8\ nm^2$. The number after the slash results from the contact area of 8.8×2.5 nm.

is barely measurable. The PS–COOH–NP, however, bind more BSA at pH values near the IEP of BSA than at more basic pH values, probably due to changing electrostatic forces.

The number of bound protein molecules per NP generally increases with decreasing protein size, which underlines again the unspecific character of the binding. If the binding mechanism had been specific, the size of the bound molecule would not have played a role, only the number of active binding sites and chemical properties on them. In addition, the linear correlation of NP mass and bound protein seems to be nonspecific.

The BSA molecules most likely adhere in a monolayer on all NP, because the bound BSA is neither sufficient for complete coverage of any of the PS–NP, nor the carbon black NP. Rezwan et al. (2004) and Röcker et al. (2009) found BSA bound in a monolayer to TiO_2 and FePt and CdSe/ZnS NP, respectively.

In case of TF, the binding of all protein molecules with their largest possible surface area is not possible on the PS–Plain–NP. Because no dimer formation of TF is denoted in the literature, we conclude that at least some proteins with smaller lateral sides adhere to the NP forming a monolayer. Apo A-1 seems to bind in a space-saving manner on PS–Plain–NP with several of the lateral sides. A monolayer of Apo A-1 is probably formed on both of the carbon black NP.

Conclusion

Our study adds to the growing information that size and surface modifications of NP essentially determine protein binding to NP in body fluids such as ELF in the lungs or blood. Our results suggest that the formation of conjugates of these three proteins, BSA, TF, and Apo A-1 with NP may be important determinants of NP translocation across cellular and organ membranes and the biokinetic fate of the NP in the body.

Acknowledgments

We are grateful for the technical assistance of Carola Eggert and Franz Erbe.

Declaration of interest

This work was partially supported by the US-National Institutes of Health, NIH grant HL074022, by the German Research Foundation (DFG) grants FOR627 and SPP1313, by EU FP6 project Particle-Risk contract No. 012912 (NEST), and by EU FP7 project NeuroNano, NMP4-SL-2008–214547.

References

Abramhoff MD, Magelhaes PJ, Ram SJ. 2004. Image processing with image. J Biophotonics Int 11:36–42.

Barrett EG, Johnston C, Oberdörster G, Finkelstein JN. 1999. Silica binds serum proteins resulting in a shift of the dose-response for silica-induced chemokine expression in an alveolar type II cell line. Toxicol Appl Pharmacol 161:111–122.

Borm PJ, Robbins D, Haubold S, Kuhlbusch T, Fissan H, Donaldson K, Schins R, Stone V, Kreyling W, Lademann J, Krutmann J, Warheit D, Oberdorster E. 2006. The potential risks of nanomaterials: a review carried out for ECETOC. Part Fibre Toxicol 3:11.

Brown DM, Stone V, Findlay P, MacNee W, Donaldson K. 2000. Increased inflammation and intracellular calcium caused by ultrafine carbon black is independent of transition metals or other soluble components. Occup Environ Med 57:685–691.

Carter DC, Ho JX. 1994. Structure of serum albumin. Adv Protein Chem 45:153–203.

Cedervall T, Lynch I, Foy M, Berggård T, Donnelly SC, Cagney G, Linse S, Dawson KA. 2007. Detailed identification of plasma proteins adsorbed on copolymer nanoparticles. Angew Chem Int Ed Engl 46:5754–5756.

Cornelius RM, Archambault J, Brash JL. 2002. Identification of apolipoprotein A-I as a major adsorbate on biomaterial surfaces after blood or plasma contact. Biomaterials 23:3583–3587.

Deng ZJ, Mortimer G, Schiller T, Musumeci A, Martin D, Minchin RF. 2009. Differential plasma protein binding to metal oxide nanoparticles. Nanotechnology 20:455101.

Donaldson K, Stone V, Tran CL, Kreyling W, Borm PJ. 2004. Nanotoxicology. Occup Environ Med 61:727–728.

Ferrer ML, Duchowicz R, Carrasco B, de la Torre JG, Acuña AU. 2001. The conformation of serum albumin in solution: a combined phosphorescence depolarization-hydrodynamic modeling study. Biophys J 80:2422–2430.

Geiser M, Rothen-Rutishauser B, Kapp N, Schürch S, Kreyling W, Schulz H, Semmler M, Im Hof V, Heyder J, Gehr P. 2005. Ultrafine particles cross cellular membranes by nonphagocytic mechanisms in lungs and in cultured cells. Environ Health Perspect 113:1555–1560.

Guex N, Peitsch MC. 1997. SWISS-MODEL and the Swiss-PdbViewer: an environment for comparative protein modeling. Electrophoresis 18:2714–2723.

Kondo A, Oku S, Higashitani K. 1991. Structural changes in protein molecules adsorbed on ultrafine silica particles. J Colloid Interface Sci 143:214–221.

Kreyling WG, Möller W, Semmler-Behnke M, Oberdörster G. 2007. Particle dosimetry: deposition and clearance from the respiratory tract and translocation towards extra-pulmonary sites. In: Particle Toxicology (Donaldson K, Borm P, eds.), CRC Press, Taylor & Francis Group, pp. 47–74.

Kreyling WG, Semmler-Behnke M, Möller W. 2006. Ultrafine particle-lung interactions: does size matter? J Aerosol Med 19:74–83.

Kreyling WG, Semmler M, Erbe F, Mayer P, Takenaka S, Schulz H, Oberdörster G, Ziesenis A. 2002. Translocation of ultrafine insoluble iridium particles from lung epithelium to extrapulmonary organs is size dependent but very low. J Toxicol Environ Health Part A 65:1513–1530.

Lottspeich F, Zorbas H. 1998. Bioanalytik. Spektrum Akademischer Verlag.

Lundqvist M, Stigler J, Elia G, Lynch I, Cedervall T, Dawson KA. 2008. Nanoparticle size and surface properties determine the protein corona with possible implications for biological impacts. Proc Natl Acad Sci USA 105:14265–14270.

Noël-Georis I, Bernard A, Falmagne P, Wattiez R. 2002. Database of bronchoalveolar lavage fluid proteins. J Chromatogr B Analyt Technol Biomed Life Sci 771:221–236.

Oberdörster G, Oberdörster E, Oberdörster J. 2005. Nanotoxicology: an emerging discipline evolving from studies of ultrafine particles. Environ Health Perspect 113:823–839.

Oberdörster G, Sharp Z, Atudorei V, Elder A, Gelein R, Lunts A, Kreyling W, Cox C. 2002. Extrapulmonary translocation of ultrafine carbon particles following whole-body inhalation exposure of rats. J Toxicol Environ Health Part A 65:1531–1543.

Oliva FY, Avalle LB, Cámara OR, De Pauli CP. 2003. Adsorption of human serum albumin (HSA) onto colloidal TiO2 particles, Part I. J Colloid Interface Sci 261:299–311.

Olivier J, Vauthier C, Taverna M, Ferrier D, Couvreur P. 1995. Preparation and characterisation of biodegradable poly(isobutylcyano acrylate) nanoparticles with the surface modified by the adsorption of proteins. Colloids Surfaces B Biointerfaces 4:4349–4356.

Peters A, Veronesi B, Calderón-Garcidueñas L, Gehr P, Chen LC, Geiser M, Reed W, Rothen-Rutishauser B, Schürch S, Schulz H. 2006. Translocation and potential neurological effects of fine and ultrafine particles a critical update. Part Fibre Toxicol 3:13.

Peters TJ. 1996. All about Albumin: Biochemistry, Genetics, and Medical Applications: Biochemistry, Genetics and Medical Applications. Academic Press San Diego Inc., San Diego, CA.

Pieper R, Gatlin CL, Makusky AJ, Russo PS, Schatz CR, Miller SS, Su Q, McGrath AM, Estock MA, Parmar PP, Zhao M, Huang ST, Zhou J, Wang F, Esquer-Blasco R, Anderson NL, Taylor J, Steiner S. 2003. The human serum proteome: display of nearly 3700 chromatographically separated protein spots on two-dimensional electrophoresis gels and identification of 325 distinct proteins. Proteomics 3:1345–1364.

Quinlan GJ, Martin GS, Evans TW. 2005. Albumin: biochemical properties and therapeutic potential. Hepatology 41:1211–1219.

Rezwan K, Meier LP, Rezwan M, Vörös J, Textor M, Gauckler LJ. 2004. Bovine serum albumin adsorption onto colloidal Al2O3 particles: a new model based on zeta potential and UV-vis measurements. Langmuir 20:10055–10061.

Röcker C, Pötzl M, Zhang F, Parak WJ, Nienhaus GU. 2009. A quantitative fluorescence study of protein monolayer formation on colloidal nanoparticles. Nat Nanotechnol 4:577–580.

Semmler M, Regula J, Oberdörster G, Heyder J, Kreyling WG. 2004. Lung-lining fluid proteins bind to ultrafine insoluble particles: a potential way for particles to pass air-blood barrier of the lung? Eur Resp J 24(Suppl.) 48100s.

Sun H, Li H, Sadler PJ. 1999. Transferrin as a metal ion mediator. Chemical Reviews 99:2817–2842.

Yang PH, Sun X, Chiu JF, Sun H, He QY. 2005. Transferrin-mediated gold nanoparticle cellular uptake. Bioconjug Chem 16:494–496.